

Iridium Containing Honeycomb Delafossites by Topotactic Cation Exchange

Supplemental Material

John H. Roudebush¹, K. A. Ross^{2,3,4}, and R. J. Cava¹

¹Department of Chemistry, Princeton University, Princeton NJ 08544 USA

²Institute for Quantum Matter, Johns Hopkins University, Baltimore MD, 21218 USA

³NIST Center for Neutron Research, Gaithersburg MD 20899 USA

⁴Current address: Colorado State University, Fort Collins CO, 80523 USA

Supplemental Table S1: Crystallographic data for $\text{Cu}_3\text{LiIr}_2\text{O}_6$ at 295 K. Space group $C2/c$, $a = 5.2910(2)$, $b = 9.1434(5)$, $c = 11.6203(5)$, $\beta = 98.798(8)$, $555.55(4) \text{ \AA}^3$. Parameters = 27. Powder X-ray diffraction: $\lambda = \text{CuK}\alpha$, $5\text{-}110^\circ 2\theta$, data points = 5245, reflections = 401. Agreement factors: $R_{\text{bragg}} = 19.6$, $R_f = 13.7$, $\chi^2 = 3.87$.

Atom	Position	x	y	z	B	Occ
Cu1	4e	0	0.728(3)	$\frac{1}{4}$	1.5	1
Cu2	4e	0	0.454(3)	$\frac{1}{4}$	1.5	1
Cu3	4e	$\frac{1}{2}$	0.581(3)	$\frac{1}{4}$	1.5	1
Ir1	8f	0.238(1)	0.078(1)	0.003(1)	0.5	0.79(1)
Li1	8f	0.238(1)	0.078(1)	0.003(1)	0.5	0.21(1)
Ir2	4d	$\frac{1}{4}$	$\frac{3}{4}$	0	0.5	0.57(1)
Li2	4d	$\frac{1}{4}$	$\frac{3}{4}$	0	0.5	0.43(1)
O1	8f	0.44(1)	0.224(7)	0.084(3)	0.93	1
O2	8f	1.01(1)	0.487(5)	0.100(5)	0.93	1
O3	9f	0.45(1)	0.566(7)	0.091(4)	0.93	1

Supplemental Table S2: Crystallographic data for $\text{Cu}_3\text{NaIr}_2\text{O}_6$, 295 K. Space group $C2/m$, $a = 5.39017(19)$, $b = 9.29984(36)$, $c = 5.97093(20)$, $\beta = 107.6399(36)$, $285.24(2) \text{ \AA}^3$. Parameters = 23. Powder X-ray diffraction: $\lambda = \text{CuK}\alpha$, $5-110^\circ 2\theta$, data points = 5251, reflections = 238, parameters. Agreement factors: $R_{\text{Bragg}} = 8.50$ $R_f = 7.27$. Powder neutron diffraction: $\lambda = 1.5398$, $13-156^\circ 2\theta$, data points = 3296, reflections = 342. Agreement factors: $R_{\text{Bragg}} = 10.8$ $R_f = 8.71$. Global $\chi^2 = 1.42$.

Atom	Position	x	y	z	B	Occ
Cu1	2c	0	0	$\frac{1}{2}$	1.9(1)	1
Cu2	4h	0	0.340(2)	$\frac{1}{2}$	1.9(1)	1
Ir1	4g	0	0.160(1)	0	0.54(1)	0.57(3)
Na1	4g	0	0.160(1)	0	0.54(1)	0.43(3)
Ir2	2b	0	$\frac{1}{2}$	0	0.54(1)	0.85(3)
Na2	2b	0	$\frac{1}{2}$	0	0.54(1)	0.15(3)
O1	8j	0.881(2)	0.343(2)	0.172(2)	0.8(1)	1
O2	4i	0.916(3)	0	0.183(4)	0.8(1)	1

Table S3: Crystallographic data for $\text{Cu}_3\text{NaIr}_2\text{O}_6$ at 5 K. Space group $C2/c$, $a = 5.3882(1)$, $b = 9.2908(2)$, $c = 11.5196(2)$, $\beta = 99.050(3)$, $V = 569.50(2) \text{ \AA}^3$. $B_{0v} = -0.52(1)$, parameters = 21. Powder neutron diffraction: $\lambda = 1.5406$, $13-156^\circ 2\theta$, data points = 3296, reflections = 642. Agreement factors: $R_{\text{bragg}} = 9.15$, $R_f = 7.75$, $\chi^2 = 2.37$. B^* and Occ^* are fixed to the values obtained for the refinement at RT, a universal B factor (B_{0v}) is used to compensate for changes in thermal parameters.

Atom	Position	x	y	z	B^*	Occ^*
Cu1	4e	0	0.757(2)	$\frac{1}{4}$	1.5	1
Cu2	4e	0	0.421(2)	$\frac{1}{4}$	1.5	1
Cu3	4e	$\frac{1}{2}$	0.593(1)	$\frac{1}{4}$	1.5	1
Ir1	8f	0.254(2)	0.080(1)	0.004(1)	0.51	0.76
Na1	8f	0.254(2)	0.080(1)	0.004(1)	0.51	0.24
Ir2	4d	$\frac{1}{4}$	$\frac{3}{4}$	0	0.51	0.52
Na2	4d	$\frac{1}{4}$	$\frac{3}{4}$	0	0.51	0.48
O1	8f	0.440(3)	0.237(2)	0.088(1)	0.93	1
O2	8f	0.941(3)	0.422(2)	0.080(1)	0.93	1
O3	9f	0.462(3)	0.576(2)	0.095(1)	0.93	1

Table S4: Unit cell refinements in C2/m of $\text{Cu}_3\text{NaIr}_2\text{O}_6$ and $\text{Cu}_3\text{Li}_2\text{IrO}_6$ as well as Na_2IrO_3 and Li_2IrO_3 . Interlayer spacing and Ir-Ir distances are also given. All units in Å, unless otherwise noted.

Phase	Instrument	temp	Space group	a	b	c	beta	layer spacing	Ir-Ir dis	ref
Na_2IrO_3	SXRD	RT	C2/m	5.4270(1)	9.395(1)	5.614(1)	109.037(18)	5.307(1)	3.130(7) 3.138(14)	1
$\text{Cu}_3\text{NaIr}_2\text{O}_6$	NPD + PXRD	RT	C2/m	5.3902(2)	9.2998(4)	5.9709(2)	108.640 (4)	5.6902(2)	3.080(5) 3.159(11)	this work
$\text{Cu}_3\text{NaIr}_2\text{O}_6$	NPD	5 K	C2/m	5.3759(2)	9.3136(3)	5.9720(1)	107.757(2)	5.6875(1)	3.097(4) 3.118(6)	this work
Li_2IrO_3	PXRD	RT	C2/m	5.1633(2)	8.9290(3)	5.1219(2)	109.759(3)	4.8203(1)	2.973(3) 2.979(1)	O'Mally
$\text{Cu}_3\text{LiIr}_2\text{O}_6$	PXRD	RT	C2/m	5.2908(3)	9.1463(5)	6.0114(2)	107.198(5)	5.7426(2)	3.041(4) 3.078(6)	this work

Table S5: Bond lengths and angles of $\text{Cu}_3\text{NaIr}_2\text{O}_6$ (s.g. = C2/m) at room temperature and 5 K

Phase	radiation	temp	Ir-Ir dis “ Ir-Ir mean, STD, % dev	Ir-O1 Ir-O2 Ir-O avg, STD, % dev	Na-O1 Na-O2 Na-O avg, STD, % dev	Ir-O1-Ir Ir-O2-Ir Ir-O-Ir avg
$\text{Cu}_3\text{NaIr}_2\text{O}_6$	Neutron +X-ray	RT	3.080(5) 3.159(11) 3.12 +/- 0.06, 1.8%	1.999(9), 2.181(15) 1.980(13) 2.053 +/- 0.11, 5.3%	2.001(12) 2.176(13) 2.089 +/- 0.12, 5.7%	97.7(4) 98.5(3) 98.1
$\text{Cu}_3\text{NaIr}_2\text{O}_6$	Neutron	5 K	3.097(4) 3.118(6) 3.108 +/- 0.15, 4.8%	2.016(6), 2.154(8) 2.046(8) 2.072 +/- 0.073, 3.5%	1.946(6) 2.157(8) 2.052 +/- 0.15, 7.3%	96.71(15) 97.5(3) 97.1

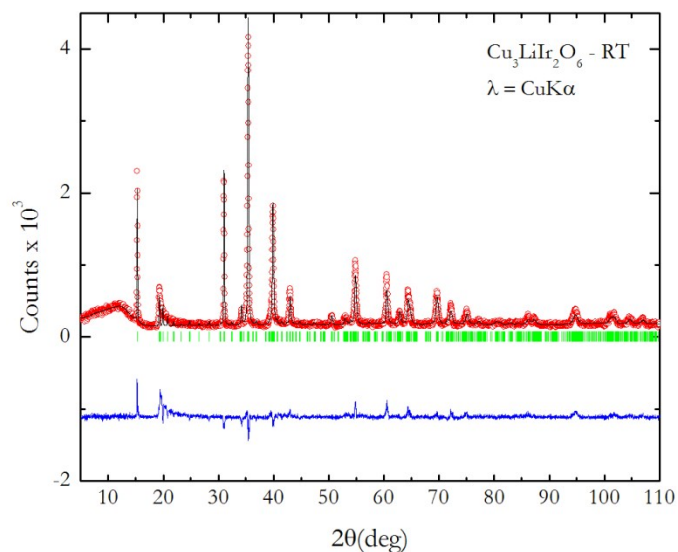


Figure S1: Powder X-ray diffraction pattern and Rietveld fit of $\text{Cu}_3\text{LiIr}_2\text{O}_6$ at room temperature in space group $C2/c$. Data is given as red circles, the fit as a black line, the difference as a blue line and Bragg reflections as green hashes.

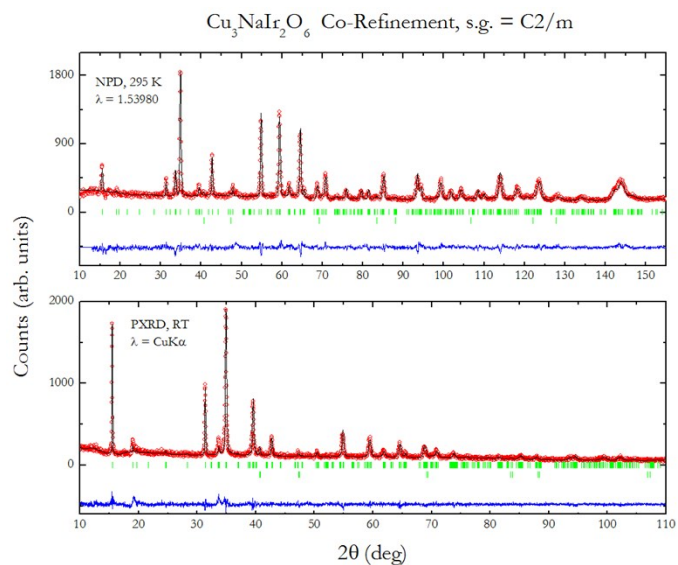


Figure S2: Neutron (upper panel) and X-ray (lower panel) powder diffraction of $\text{Cu}_3\text{NaIr}_2\text{O}_6$ (s.g. = $C2/m$) at 295 K with Rietveld fit. Data is given as red circles, the fit as a black line, the difference as a blue line and Bragg reflections as green hashes.

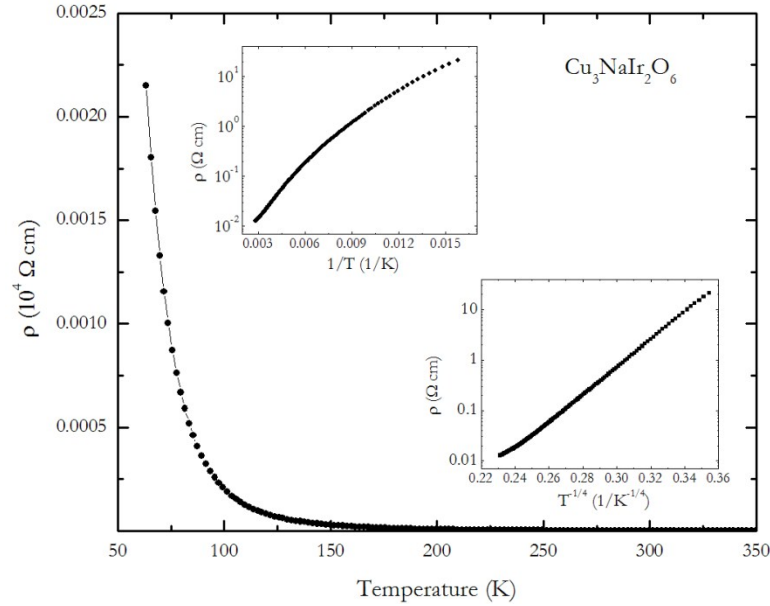


Figure S3: Resistivity ρ ($\Omega \cdot \text{cm}$), of $\text{Cu}_3\text{NaIr}_2\text{O}_6$ from 350 to 65 K measured upon cooling. Upper left inset - log plot of ρ vs. $1/T$. The data cannot be fitted to an activated Arrhenius behavior $\rho(T) = \exp(-\Delta/T)$. Lower right inset - log plot of ρ vs. $1/T^{-1/4}$ allowing for a good fit to an activated $\rho(T) = \exp[-(\Delta/T)^{1/4}]$ associated with a variable-range hopping mechanism and similar to Na_2IrO_3 . {Singh, 2010 #930}

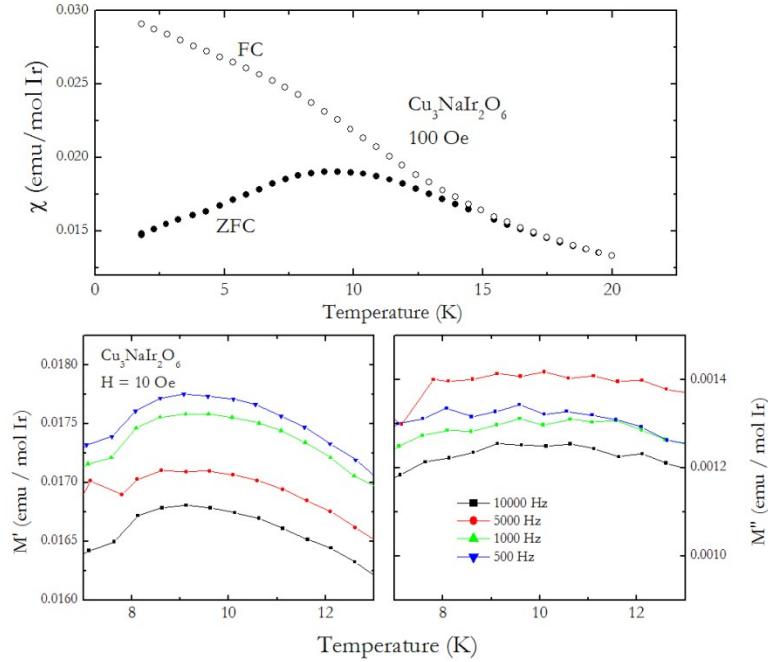


Figure S4: Upper – Field cooled (FC) and zero-field cooled (ZFC) magnetization of $\text{Cu}_3\text{NaIr}_2\text{O}_6$ measured with an applied field of 100 Oe. Lower – AC magnetization, real M' (Left) and imaginary (right) portions of the signal in the temperature range of the magnetic transition. Samples were measured with a 10 Oe applied field and 500, 1000, 5000 and 10,000 Hz. A change in the transition temperature with frequency, a classic characteristic of a spin-glass, is not observed.

1. Choi, S. K.; Coldea, R.; Kolmogorov, A. N.; Lancaster, T.; Mazin, I. I.; Blundell, S. J.; Radaelli, P. G.; Singh, Y.; Gegenwart, P.; Choi, K. R.; Cheong, S. W.; Baker, P. J.; Stock, C.; Taylor, J., Spin waves and revised crystal structure of honeycomb iridate Na_2IrO_3 . *Phys Rev Lett* **2012**, 108, (12), 127204.